displaced partner in the ⟨110⟩ direction were a fluorine the hole would tend to be concentrated on it, rather than on the adjoining bromine or chlorine which will occupy as nearly as possible normal lattice sites. This conclusion is in accord also with the fact that the binding of BrF and ClF molecules is 30% weaker than that of the Cl_2^- molecule, which implies that the corresponding $(XY)^-$ molecules are also more weakly bound than the Cl_2^- molecule. It follows that the binding effects due to the spread of the hole along the ⟨110⟩ direction would be weak or even totally absent and the ⟨111⟩ direction would be preferred as discussed above. This is in agreement with experiment.

ACKNOWLEDGMENTS

It is a pleasure to acknowledge our indebtedness to Dr. Wahl and Dr. Gilbert at Argonne National Laboratory for supplying the interaction potential for the Cl_2^-. We also wish to thank Dr. Ralph Bartram for a discussion of the effects of crystal-field symmetry and William D. Wilson for performing some of the calculations.

PHYSICAL REVIEW VOLUME 157, NUMBER 3 15 MAY 1967

Electromodulation of the Optical Constants of Rutile in the uv

A. FROVA,† P. J. BODDY, AND Y. S. CHEN
Bell Telephone Laboratories, Murray Hill, New Jersey
(Received 6 December 1966)

Large light modulation has been achieved at room temperature by electroreflectance in single-crystal and by electroabsorption in polycrystalline TiO_2. The behavior is similar to that exhibited by some of the perovskite-type ferroelectrics, for instance, barium titanate, but cannot be explained by a shift of the energy levels as found in the case of potassium tantalate. The observed effects have been accounted for in terms of a strongly lifetime-broadened Franz-Keldysh tunneling, with small additional shifts of the critical points, occurring upon application of the electric field. From the electroreflectance spectra, critical points in the optical constants have been detected in good agreement with those known from absolute reflectance data. A correlation of the data with the band structure of rutile has been attempted. Spectra from polycrystalline material do not show great differences from those of single crystals.

INTRODUCTION

TWO of the authors have recently reported[1,2] electroreflectance (hereafter referred to as ER) and electroabsorption (EA) measurements in some ferroelectric materials having perovskite structure (e.g., $KTaO_3$ and $BaTiO_3$). As opposed to germanium, silicon, III-V and II-VI compounds, and other materials,[3–6] where optical field effects can usually be accounted for in terms of just Franz-Keldysh photon-assisted tunneling, in $KTaO_3$ actual shifts and splittings of certain band-structure critical points with electric field have been observed. In particular, a large field dependence was observed in the main reflectivity peak (between 4 and 5 eV for most investigated materials[7]), which corresponds approximately to the position of a classical oscillator chosen to fit the refractive-index dispersion below the fundamental energy gap. We have shown[2] that the large electro-optic effect observed in the visible in some ferroelectric materials[8] is a consequence of the above-mentioned optical field effects in the uv. Because of the large ionic and electronic polarizabilities of the transition-metal ion in ferroelectric materials having perovskite structure,[9] we interpreted the observed behavior of $KTaO_3$ as being at least in part due to changes in the overlap integrals of the transition-metal–oxygen pairs, which affect the band-structure critical points up to energies much higher than those explored in our experiments.[10]

The reason for our interest in investigating rutile (TiO_2) is that, although it does not appear to be ferroelectric over the range of temperatures from 1.6 to 1060°K, its ionic polarizability is very close to that needed for the polarization catastrophe to take place.[11] Local fields at lattice sites, when the Ti ion is ionically polarized, have been calculated to be comparable to

† Present address: Istituto di Fisica dell' Università di Roma, Rome, Italy.

[1] A. Frova and P. J. Boddy, Phys. Rev. Letters **16**, 688 (1966).
[2] A. Frova and P. J. Boddy, Phys. Rev. **153**, A606 (1967).
[3] A. Frova, P. Handler, F. Germano, and D. E. Aspnes, Phys. Rev. **145**, 575 (1966).
[4] B. O. Seraphin, R. B. Hess, and N. Bottka, J. Appl. Phys. **36**, 2242 (1965); B. O. Seraphin, Phys. Rev. **140**, A1716 (1965).
[5] K. L. Shaklee, F. H. Pollak, and M. Cardona, Phys. Rev. Letters **15**, 883 (1965); *ibid.* **16**, 48 (1966).
[6] R. Williams, Phys. Rev. **126**, 442 (1962).
[7] M. Cardona, Phys. Rev. **140**, A651 (1965).
[8] F. S. Chen, J. E. Geusic, S. K. Kurtz, J. C. Skinner, and S. H. Wemple, J. Appl. Phys. **37**, 388 (1966), and references therein.
[9] J. C. Slater, Phys. Rev. **78**, 748 (1950); S. Triebwasser, J. Phys. Chem. Solids **3**, 53 (1957).
[10] A. H. Kahn and A. J. Leyendecker, Phys. Rev. **135**, A1321 (1964).
[11] R. A. Parker, Phys. Rev. **124**, 1713 (1961); *ibid.* **124**, 1719 (1961).

those characteristic of barium titanate. Moreover, the environment of the Ti ion in rutile consists of somewhat distorted TiO_6 octahedra, this structure being the basic constituent of the perovskite-type ferroelectrics. For these reasons we expect the band structure and the ER behavior of rutile to be somewhat similar to that of the titanates. In fact, the first absorption edges of TiO_2,[12] $BaTiO_3$,[13] and $SrTiO_3$,[14] presumably due to $O(2p)$–$Ti(3d)$ transitions, occur at approximately the same energy (≈ 3 eV), and their absolute reflectivity spectra[7] present some similarities.

After a brief description of the experimental method in the first part of the paper, the results of ER in single crystals are reported in Sec. II, and the main features of the spectra are compared with the behavior of the perovskite ferroelectrics. In Sec. III, the separate contributions to the ER of the real and imaginary parts of the dielectric constant are calculated, and singularity points in the optical constants are compared with those previously known from absolute reflectivity experiments.[15] The results of EA in anodically grown TiO_2 are reported in Sec. IV. Finally, Sec. V is devoted to a discussion of the observed effects. A theoretical fit to the experimental data is obtained by introducing parametrically a lifetime-broadening term in the theory of the Franz-Keldysh effect.

I. EXPERIMENTAL

The experimental apparatus used for the present measurements has been described in detail in a previous paper.[2] A sample-liquid electrode arrangement was used to apply large dc electric fields and small ac modulating voltages; the ac voltage was kept at about 10% of the dc bias to ensure linearity in the signal. The ratio of the field-modulated reflectance to the total reflectance was directly recorded as a function of wavelength. Rutile samples of about $3\times2\times2$ mm^3 were cut from a large boule of material grown by the flame-fusion technique. The specimens were oriented by x-ray diffraction to have the long edge parallel to the c axis and the other two edges perpendicular to it. All faces were optically polished with 0.05-μ Linde B powder, and data were taken on faces both parallel and perpendicular to the c axis. Samples with various donor concentrations, ranging from 10^{18} to 5×10^{19} per cc, were obtained by oxygen reduction in hydrogen atmosphere at temperatures between 700 and 800°C. Although the crystal showed a uniform coloration, indicating that the oxygen vacancy concentration was rather uniform throughout the crystal, it is believed that in some cases the surface region had a somewhat different donor density from the bulk. For instance, faces perpendicular to the c axis appeared to increase their doping upon polishing. In particular,

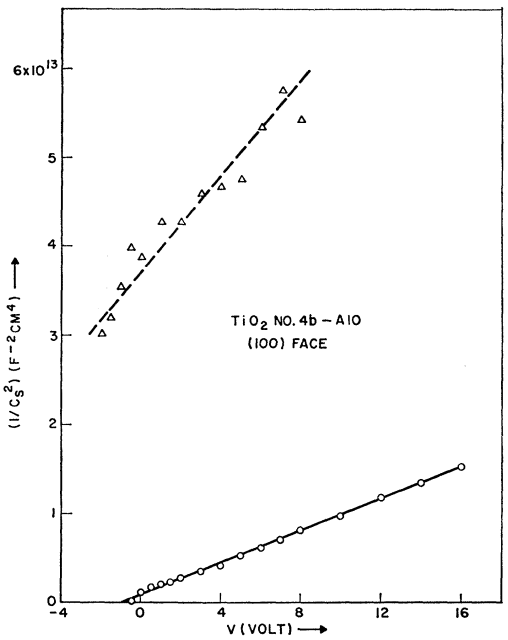

FIG. 1. Sample-electrolyte interfacial capacitance per unit area before (circles) and after (triangles) oxygen evolution at the interface.

electrochemical evolution of oxygen at the sample surface when a high reverse voltage was applied produced a reduction of the vacancy concentration near the surface and caused the field to shift to lower values; this appeared as a gradual decrease of the ER signal in time. The effect was negligible at lower applied voltages, where most of the data were obtained. Similar effects were observed by measurement of sample-electrolyte interfacial capacitance, which is practically the semiconductor space-charge capacitance. Figure 1 illustrates the dependence of such capacitance (measured differentially by a pulse technique[16]) on the reverse voltage for a (100) face immediately after the sample had been immersed in the electrolyte (circles) and after it had been subjected to a reverse current of the order of 1 mA for 30 min (triangles). The straight line in the former case indicates that the donor concentration

$$N_d=\frac{2}{\epsilon\epsilon_0 q}\left[\frac{d(1/C_s^2)}{dV}\right]^{-1},$$

(where $\epsilon\epsilon_0$ is the dielectric permittivity and C_s is the capacitance per unit area) is uniform and equal to 1.4×10^{18} cm^{-3}, while in the latter case the data show that a layer of lower donor density (4.8×10^{17}) has developed at the surface. This effect could be reversed by biasing the sample in the forward direction evolving hydrogen at the crystal surface, or by heating the sample in inert atmosphere. An attempt was made to measure the donor density prior to immersion of the

[12] P. Moch, M. Balkanski, and P. Aigrain, Compt. Rend. **251**, 1373 (1960).
[13] R. C. Casella and S. P. Keller, Phys. Rev. **116**, 469 (1959).
[14] J. A. Noland, Phys. Rev. **116**, 1469 (1959).
[15] M. Cardona and G. Harbeke, Phys. Rev. **137**, A1467 (1965).
[16] W. H. Brattain and P. J. Boddy, J. Electrochem. Soc. **109**, 574 (1962).

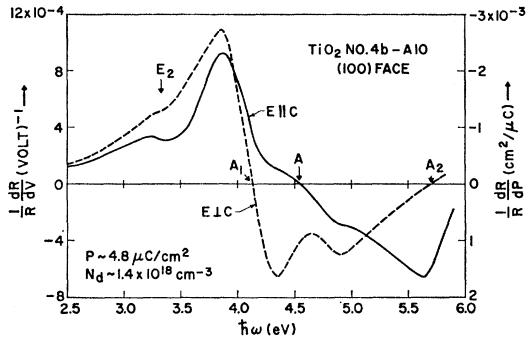

FIG. 2. ER for a (100) face with light polarized, respectively, parallel and normal to the c axis. The sign of $(1/R)(dR/dV)$ has been chosen positive for reflectance decreasing upon increase of the electric field. Surface field $F_S \sim 6\times10^5$ V/cm.

sample in the electrolyte by evaporating gold dots onto the surface and by measuring the Schottky-barrier capacitance. We found, in general, that the donor concentration appeared to be a few times larger than that measured in the sample-electrolyte system. Since in rutile oxygen can be easily diffused out by heating in vacuum, we attributed this fact to the formation of a highly oxygen-deficient region under the metal dots, due to the rather high temperature attained locally during vacuum evaporation. For the above-mentioned reasons, control of impurity concentration during the experiment was difficult and the surface field and polarization at the various bias voltages could be determined only with considerable uncertainty. For best spectral resolution, the data were generally taken at the lowest possible dc field. This limit was set by the doping of the sample and/or by the requirement that the signal were at least an order of magnitude larger than the noise.

II. ELECTROREFLECTANCE RESULTS IN SINGLE CRYSTALS

Data were taken in a number of samples, and the results were well reproducible. Figures 2 through 4 show the room-temperature ER spectra, at nearly normal incidence, of reduced single-crystal rutile. The curves illustrated are rather typical, their shape varying only slightly with the magnitude of both the dc and the ac field. In particular, field-on–field-off measurements yielded approximately the same spectra as the differential ER. The figures in order refer to a (100) face, (110) face, both containing the c axis, and to a (001) face (perpendicular to the c axis). In the first two cases, data for light polarized parallel and perpendicular to the c axis are shown. The upper energy limit was determined by the cutoff of the electrolyte and of the CaF_2 polarizer. Taking the reverse voltage V with minus sign, the sign of the ER, defined as $(1/R)(dR/dV)$, has been chosen positive for R decreasing upon an increase of the electric field. This convention has been maintained throughout the paper. The spectra have many similarities with those of the perovskite ferroelectrics.[1,2] The following features should be stressed:

(a) The magnitude of the ER is remarkably large; use of an ac voltage equal to twice the dc bias and large enough to approach breakdown in the reverse half-wave resulted in about 25% light modulation at the major positive peak and more than 5% below the absorption threshold.

(b) The spectra do not appear as sharp lines located at each of the critical points, being zero elsewhere, as would be expected for a normal Franz-Keldysh-type photon-assisted tunneling. The ER rather consists of broad bands, with just one or two zeros located at the energies of the main peaks of the total reflectivity curves (see Ref. 15).

(c) Unlike $KTaO_3$, but in agreement with the behavior of $BaTiO_3$,[2] rather small shifts of the ER zeros [at most 50 meV (millielectron volts)] were observed when the field was varied over a wide range. In Fig. 3, for instance, the 4-eV null of the dashed curve was

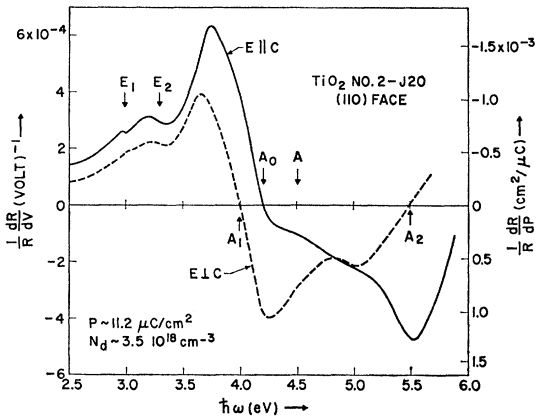

FIG. 3. ER for a (110) face (containing the c axis). Surface field $F_S \sim 10^6$ V/cm.

found to move slightly to lower energies for increasing fields up to a certain value, and then to shift back towards its initial position. Since the general shape and the sign of the ER were practically independent of this effect, we believe that the spectra cannot be explained in terms of simple critical-point shifts.

(d) Within the uncertainty in the determination of the surface polarization P and the requirement of keeping the field low to avoid oxygen evolution, the magnitude of $(1/R)(dR/dP)$ at the peaks appeared to be nearly independent of the applied field. This suggests that for not too large reflectance changes, $R(P)-R(0)$ is roughly linear with polarization. Figures 2–4 can therefore be directly compared in order to estimate the relative magnitude of the effect for the various field and light polarization orientations. At the positive peak, $(1/R)(dR/dP)$ is approximately equal for all cases. Comparison of Fig. 2 (field applied along the a axis) with Fig. 3 (field applied along a ⟨110⟩ direction normal

to the c axis) shows that the direction of the induced polarization is an important factor in determining the shape of the ER spectra.

One would be tempted to correlate directly the observed structure in the ER (zeros and inflection points) with the band-structure critical points. In reality, the overlapping of the contributions of $d\epsilon_1/dV$ and $d\epsilon_2/dV$, with ϵ_1 and ϵ_2 being, respectively, the real and imaginary part of the dielectric constant, may generate accidental structure in dR/dV. In Sec. III, before proceeding to a discussion of the experimental results, we intend to separate these terms by application of the Kramers-Kronig dispersion relation between reflectivity and phase.

III. CRITICAL POINTS IN THE OPTICAL CONSTANTS

If we represent the complex amplitude of reflection r by $r=R^{1/2}e^{i\varphi}$, the phase angle φ is related to the reflectivity R through the Kramers-Kronig relation (see, e.g., Ref. 17)

$$\varphi(\omega)=-\frac{\omega}{\pi}\int_0^\infty \frac{\ln R}{\omega'^2-\omega^2}d\omega',$$

and by differentiation with respect to an applied voltage,

$$\frac{d\varphi(\omega)}{dV}=-\frac{\omega}{\pi}\int_0^\infty \frac{1}{R}\frac{dR}{dV}\frac{d\omega'}{\omega'^2-\omega^2}. \tag{1}$$

Since Eq. (1) calls for integration from 0 to ∞, there is a general reluctance to apply Kramers-Kronig relations when the optical data cover a rather narrow range of energies. However, when dealing with a differential experiment that yields a series of positive and negative oscillations, whose contributions may cancel far away from the cutoff energy, one can assume that the integrand, in this case $(1/R)(dR/dV)$, is zero at all energies above the experimental range. In our experiment, moreover, we meet the favorable condition that $(1/R)(dR/dV)$ tends to become practically a constant at energies somewhat lower than the fundamental threshold. The correctness of these assumptions can be confirmed *a posteriori* by additional arguments. With the above-mentioned approximations, the integral in Eq. (1) can be transformed into

$$\frac{d\varphi(\omega)}{dV}=\frac{1}{2\pi}\Bigg[\left(\frac{1}{R}\frac{dR}{dV}\right)_{\omega=\omega_1}\ln\frac{\omega+\omega_1}{\omega-\omega_1}-2\omega\int_{\omega_1}^{\omega-\Delta\omega}\frac{1}{R}\frac{dR}{dV}\frac{d\omega'}{\omega'^2-\omega^2}+\left(\frac{1}{R}\frac{dR}{dV}\right)_{\omega=\omega}\times\ln\frac{2\omega-\Delta\omega}{2\omega+\Delta\omega}-2\omega\int_{\omega+\Delta\omega}^{\omega_2}\frac{1}{R}\frac{dR}{dV}\frac{d\omega'}{\omega'^2-\omega^2}\Bigg],$$

where $\hbar\omega_1$ and $\hbar\omega_2$ are the limits of the experimental range, 2.5 and 6 eV, respectively. The value of $\hbar\Delta\omega$ was chosen to be 0.05 meV, resulting in an error in $d\varphi/dV$ of less than 0.1%. $d\epsilon_1/dV$ and $d\epsilon_2/dV$ can be evaluated from the experimental values of $(1/R)(dR/dV)$ and the calculated values of $d\varphi/dV$ by differentiating the equations[17]

$$\epsilon_1=\frac{(1-R)^2-4R\sin^2\varphi}{(1+R-2R^{1/2}\cos\varphi)^2}\epsilon',$$

$$\epsilon_2=\frac{4(1-R)R^{1/2}\sin\varphi}{(1+R-2R^{1/2}\cos\varphi)^2}\epsilon',$$

where ϵ' is the optical dielectric constant of the electrolyte. One obtains

$$\frac{d\epsilon_1}{dV}=A(\epsilon_1,\epsilon_2,\epsilon')\frac{1}{R}\frac{dR}{dV}+B(\epsilon_1,\epsilon_2,\epsilon')\frac{d\varphi}{dV}, \tag{2a}$$

$$\frac{d\epsilon_2}{dV}=-\tfrac{1}{2}B(\epsilon_1,\epsilon_2,\epsilon')\frac{1}{R}\frac{dR}{dV}+2A(\epsilon_1,\epsilon_2,\epsilon')\frac{d\varphi}{dV}. \tag{2b}$$

Similar equations can be derived for the real and imaginary parts of the refractive index, n and k, respectively. The coefficients A and B have been calculated using the experimental values of ϵ_1 and ϵ_2 reported by Cardona and Harbeke[15] and the values of ϵ' for water.[18] This computation was carried out for all the experimental data. The results for the cases $\mathbf{E}\|c$ and $\mathbf{E}\perp c$ of Fig. 2 are shown in Figs. 5–8. The circles in Figs. 6 and 7 represent $d\epsilon_1/dV$ as calculated from the ER data in the range where $\epsilon_2\simeq 0$, and where

$$\frac{1}{R}\frac{dR}{dV}=\frac{2}{\epsilon_1-\epsilon'}(\epsilon'/\epsilon_1)^{1/2}\frac{d\epsilon_1}{dV}.$$

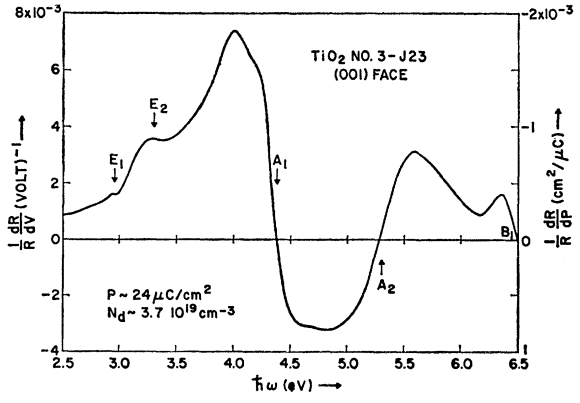

FIG. 4. ER for a (001) face (perpendicular to the c axis).

[17] F. Stern, in *Solid State Physics*, edited by F. Seitz and D. Turnbull (Academic Press Inc., New York, 1962), Vol. 15, p. 299.

[18] *International Critical Tables*, edited by E. W. Washburn (McGraw-Hill Book Company, Inc., New York, 1930), Vol. 7, p. 13.

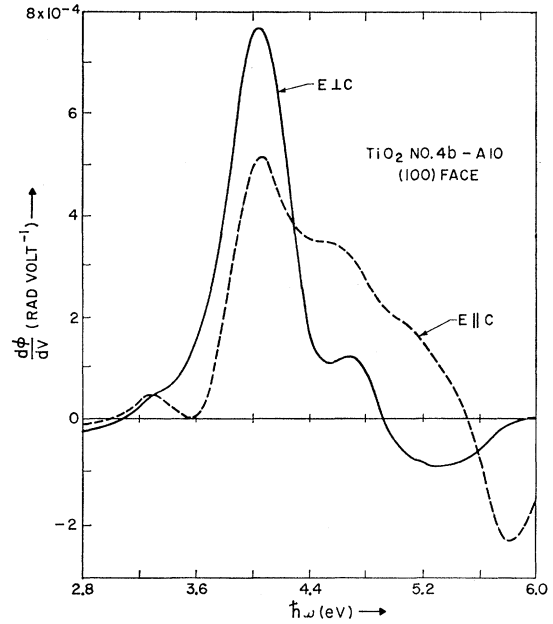

FIG. 5. Phase modulation for light polarized parallel and perpendicular to the c axis (from data of Fig. 2).

The agreement between these values and those obtained through Kramers-Kronig transformation is within 1% up to 3.5 eV, confirming, at least on the low-energy side of the spectrum, the validity of the assumptions made. Also, the vanishing of $d\epsilon_2/dV$, $d\varphi/dV$, and dk/dV for energies lower than the absorption edge at 3 eV provides

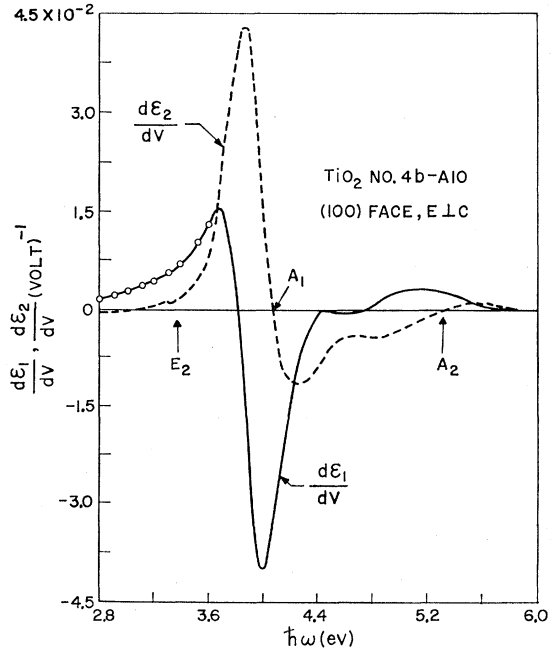

FIG. 6. Electromodulation of the real and imaginary parts of the dielectric constant for light polarized perpendicular to the c axis (from data of Fig. 2). For sign convention see caption of Fig. 2.

further evidence that our procedure was sufficiently correct.

The main features of the curves shown in Figs. 2, 6–8 plus similar data for a (110) face have been summarized in Table I. The zeros and inflections of the electromodulated R, ϵ_2, and k are compared with pertinent peaks of the same quantities available from Ref. 15. The agreement is very good and shows that the field derivative of the optical parameters behaves to some extent as their frequency derivative. We have accordingly assumed that the singularity points are located near the inflections of the $d\epsilon_2/dV$ curve.

Singularity points labeled E_1 and E_2 in Table I have not been observed before in reflectance. E_1 agrees well with the minimum energy gap observed by various authors in optical absorption,[12,19] photoconductivity[19] and transport[19,20] measurements. Recently, Arntz and

TABLE I. Singularity points in the optical parameters of rutile. Data from present experiment are compared with those obtained by Cardona and Harbeke from absolute reflectivity measurements. Energies are in eV.

Singularity	E_1	E_2	A_1	A_2	E_1	E_2	A
$\frac{1}{R}\frac{dR}{dV}$ (100)	~3.0	~3.3	4.13	5.70	···	~3.3	4.55
$\frac{1}{R}\frac{dR}{dV}$ (110)	~3.0	~3.3	3.98	5.50			
R[a]	···	···	3.97	5.52	···	···	4.60
$\frac{d\epsilon_2}{dV}$ (100)	···	~3.3	4.07	~5.35	···	~3.4	4.15
$\frac{d\epsilon_2}{dV}$ (110)	···	~3.3	3.99	~5.22			
ϵ_2[a]	···	···	4.0	5.35	···	···	4.11
$\frac{dk}{dV}$ (100)	···	~3.3	4.19	~5.58	···	~3.4	4.37
$\frac{dk}{dV}$ (110)		~3.3	4.08	~5.42			
k[a]	···	···	4.10	5.51	···	···	4.35
Light vector		$\mathbf{E}\perp c$ axis				$\mathbf{E}\parallel c$ axis	

[a] From Ref. 15.

Yacoby[21] have suggested that this is an indirect edge, slightly dichroic, the dichroism being due to a difference in the energy of the assisting phonon for $\mathbf{E}\parallel c$ or $\mathbf{E}\perp c$. The singularity point E_2, which is clearly detectable only for $\mathbf{E}\parallel c$, falls between 3.3 and 3.4 eV, an energy where a secondary photoconductivity peak has been observed by Cronemeyer.[19] The same author found that the conductivity has two activation energies, differing by 0.3 eV, respectively, below and above 1150°K. We assign E_2 to the first direct absorption edge, as will be discussed at the end of the paper. In Sec. V we intend to show also that the A_1 and A_2 singularities correspond, respectively, to M_1 and M_2 saddle-point edges, while A (for $\mathbf{E}\parallel c$) results actually from the contributions of at least two critical points.

[19] D. C. Cronemeyer, Phys. Rev. 87, 876 (1952).
[20] J. H. Becker and W. R. Hosler, Phys. Rev. 137, A1872 (1964).
[21] F. Arntz and Y. Yacoby, Phys. Rev. Letters 17, 857 (1966).

We wish to make a final remark relative to the data listed in Table I. In his birefringence studies, DeVore[22] fitted the dispersion curves of the refractive index of rutile in the visible by means of a single harmonic oscillator located at 4.27 eV for $\mathbf{E}\|c$ and 4.38 eV for $\mathbf{E}\perp c$. The former value falls very close to the A singularity of k in our experiment. The latter is somewhat between A_1 and A_2. Transitions associated with such critical points, rather than with the first absorption edge, therefore determine the optical properties of the crystal in the visible. Since these critical points are strongly affected by the electric field, one would expect rutile to exhibit a large electro-optic effect in the visible.

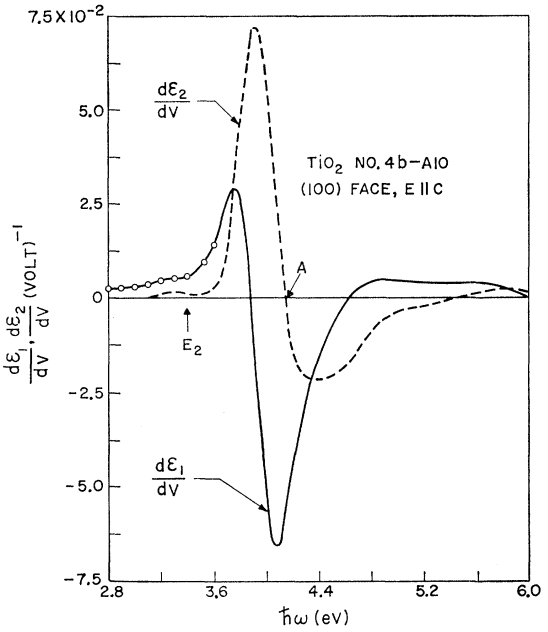

FIG. 7. Electromodulation of the real and imaginary parts of the dielectric constant for light polarized parallel to the c axis (from data of Fig. 2).

IV. ELECTROABSORPTION IN POLYCRYSTALLINE TiO_2

Large light modulation has been achieved at 3.75 eV by electric-field modulation of the optical absorption of anodically grown TiO_2. X-ray examination showed weak evidence of crystalline regions smaller than 100 Å in size. Films of about 300–500 Å were grown on evaporated layers of titanium, and the field, smaller than that required for further growth, was applied between the metal substrate and the electrolyte. Light at normal incidence passed through the TiO_2 film twice, after reflection on the Ti surface. The relative modulation was detected in the usual manner. Apparently ER effects in this case were negligible, since no light modulation was observed in the energy range where the

[22] J. R. DeVore, J. Opt. Soc. Am. **41**, 416 (1951).

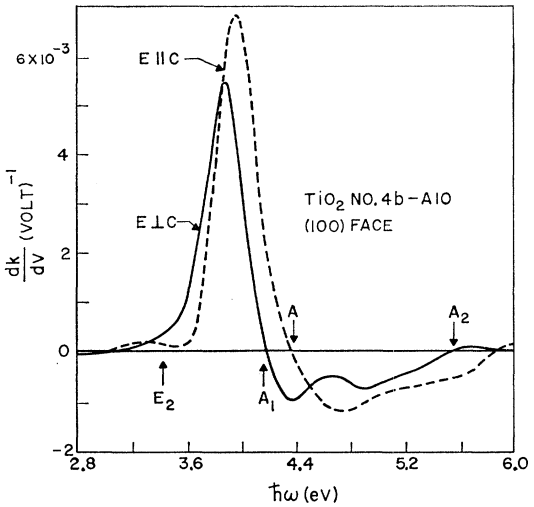

FIG. 8. Electromodulation of the absorption index (from data of Fig. 2).

absorption coefficient exceeded $\approx 5\times10^5$ cm^{-1} (approximately above 4.0 eV according to Ref. 15). This is shown in Fig. 9, where the relative light modulation per unit voltage $(1/I)(dI/dV)$ for an applied dc bias of 20 V (field $\approx 5\times10^6$ V/cm) has been plotted as a function of photon energy. $(1/I)(dI/dV)$ is directly proportional to $-\omega dk/dV$. The following features should be stressed:

(a) Light modulation at 3.75 eV for full 40-V peak-to-peak ac voltage was as high as 20%.

(b) The general shape of the EA curve is somewhat similar to those of dk/dV in Fig. 8 for the single crystal and is related to the frequency derivative of the absorption coefficient reported in Ref. 12 for amorphous material. This is consistent with the ER results.

(c) It appears from EA that the polycrystalline-material critical points occur at approximately the same energies as in single crystals. It has been shown by Breckenridge and Hosler[23] that there is no significant

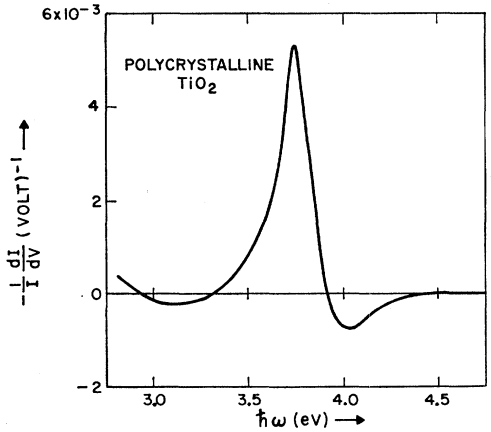

FIG. 9. Electroabsorption of polycrystalline material.

[23] R. G. Breckenridge and W. R. Hosler, Phys. Rev. **91**, 793 (1953).

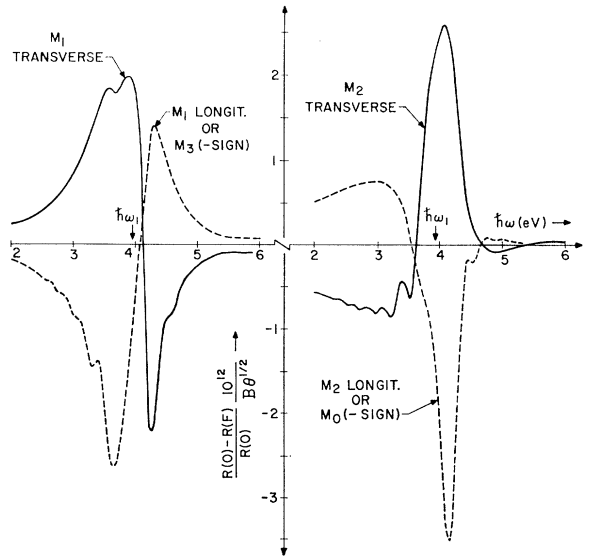

FIG. 10. Theoretical lifetime-broadened ER of rutile for $\mathbf{E}\perp c$ at critical points of various types located at $\hbar\omega_1=3.95$ eV. M_0, M_3 =parabolic thresholds, respectively, a minimum and a maximum of the interband energy. M_1, M_2 transverse (longitudinal) =saddle-point edges with the symmetry axis of the odd-sign mass perpendicular (parallel) to the electric field.

difference between single-crystal and polycrystalline material with respect to mobility, effective mass, and thermal activation energy. From the above results, it appears that a number of metal oxides can be conveniently investigated by the simple technique used in this experiment. Useful information about band structure may be easily obtained.

V. DISCUSSION

In Sec. II, we mentioned that the position of the critical points of the ER spectra was only slightly affected by the value of the dc field. The same behavior was noted in the EA of polycrystalline material. It is not possible, therefore, to explain the optical field effects in rutile in terms of displacements of the critical points, a mechanism which appeared to be largely responsible for the behavior of the tantalates.[2] In this respect, TiO_2 behaves very similarly to ferroelectric $BaTiO_3$. On the other hand, the lack of dependence of the width of the ER bands on the applied field, plus the absence of satellite oscillations in the proximity of the main peaks, seems to indicate that the simple Franz-Keldysh effect cannot account for the observed spectra. However, these characteristic features of the Franz-Keldysh effect may not be met if strong lifetime broadening effects are present. This is probably the case for rutile, where mobility is as low as 0.3 cm^2/V sec at room temperature and is entirely governed by phonon scattering.[23] For a conductivity mass of about $50m_e$,[23] this leads to a lifetime of the order of 10^{-14} sec, corresponding to a relaxation constant Γ of about 0.1 $eV/\hbar$, or even higher for electrons well above the bottom of the conduction band. As a matter of fact, the experiments of Arntz and Yacoby[21] reveal that almost no structure is found in the room temperature EA of rutile at the first absorption edge.

To include lifetime broadening effects, we have followed a procedure recently suggested by Aspnes.[24] In a generalized theory of the Franz-Keldysh effect, valid for all types of critical points, Aspnes has expressed in closed form the field-induced changes of the real and imaginary parts of the dielectric constant, including Lorentzian broadening, in terms of Airy functions of complex variable. This was done by introducing two "electro-optical functions" F and G which describe the behavior of $\Delta\epsilon_1$ and $\Delta\epsilon_2$ at any critical point of interest. These functions are given by the real and the imaginary parts of the following expression:

$$F(X_0,\Gamma/\Theta)+iG(X_0,\Gamma/\Theta)$$
$$=2\pi[e^{-i\pi/3}\,\mathrm{Ai}'(z)\,\mathrm{Ai}'(w)+w\,\mathrm{Ai}(z)\,\mathrm{Ai}(w)]$$
$$-\left[\frac{-X_0+[X_0^2+(\Gamma/\Theta)^2]^{1/2}}{2}\right]^{1/2}$$
$$+i\left[\frac{X_0+[X_0^2+(\Gamma/\Theta)^2]^{1/2}}{2}\right]^{1/2}, \quad (3)$$

where Ai is the Airy function, Γ is the relaxation constant,

$$X_0^{\pm}=\pm(\omega_1-\omega)/\Theta \quad (\hbar\omega_1=\text{critical-point energy}),$$
$$z=X_0+i\Gamma/\Theta, \quad w=ze^{-i2\pi/3},$$

and

$$\Theta=(q^2F^2/2\mu\hbar)^{1/3},$$

where F is the electric field and μ is the reduced electron-hole effective mass. Θ gives a measure of the field-induced edge spreading on the nonoscillatory side of the Airy function.

At all critical points, the field-induced changes in ϵ_1 and ϵ_2 are always given by an expression of the type

$$\Delta\epsilon_i=\pm(B\Theta^{1/2}/\omega^2)H(X_0^{\pm},\Gamma/\Theta), \quad (4)$$

where B is a constant related to the interband optical matrix element and H is either an electro-optical function of the first type F, or of the second type G. The choice of such a function and of the various signs appearing in Eq. (4) characterizes each type of critical point. An exhaustive table summarizing all cases is given in Ref. 24. In particular, for $\Gamma=0$ and X_0 taken with a plus sign, the function F leads to the familiar energy dependence of the Franz-Keldysh effect of the absorption coefficient near a parabolic threshold.[25]

We have calculated the lifetime broadened ER for all types of critical points by eliminating the phase term in Eqs. (2a) and (2b), in the limit of not too large

[24] D. E. Aspnes, Phys. Rev. **153**, A972 (1967).
[25] K. Tharmalingam, Phys. Rev. **130**, 2204 (1963).

reflectance changes. The results of this calculation, for the case $\mathbf{E}\perp c$, are shown in Fig. 10. The zero-field values of ϵ_1 and ϵ_2 have been taken from Ref. 15. The actual magnitude of the ER can be evaluated only if B is known. The calculation was performed for a number of values of Γ, Θ, and ω_1. The curves of Fig. 10 were obtained taking $\hbar\Theta=190$ meV and $\hbar\Gamma=325$ meV, values which seemed to give the best agreement with the experimental results, as will appear later. For direct comparison with theory, field-on–field-off data for a (100) face and $\mathbf{E}\perp c$ were taken by sweeping the ac voltage from zero to twice the dc bias. The experimental values of $\Delta R/R$ obtained by this procedure are shown as triangles in Fig. 11. It appears, from comparison with Fig. 10, that the experimental spectrum cannot be accounted for in the whole range by just one critical point. The structure is due to the overlapping of the contributions of two (or more) critical points. The low-energy side of the spectrum, below 4.5 eV, corresponds to the ER of an M_1 saddle-point edge with symmetry axis of the odd-sign mass perpendicular to the electric field (M_1 transverse). An M_3 threshold would also fit the data, at least qualitatively, but it is reasonable to assume that a maximum of the interband energy should not be encountered first. An M_2 transverse is a possible candidate to explain the high-energy side of the spectrum. Although contributions from M_1 and M_2 longitudinal (unless forbidden by selection rules) and from other critical points may be present, we have attempted to fit the experimental data for $\mathbf{E}\perp c$ by overlapping the contributions of an M_1 transverse saddle point located at 3.95 eV and an M_2 transverse one at 5.35 eV. These energies are rather close to the singularities of ϵ_2 determined from absolute reflectance in Ref. 15 (see Table I, case $\mathbf{E}\perp c$). The theoretical curve has been arbitrarily normalized to coincide with experiment at the 3.85-eV positive peak and at the 4.85-eV negative peak of the spectrum. In view of the rather drastic approximations made in assuming that Aspnes's theory is still valid far away from the critical points and that Γ and μ at each edge are constant throughout all energies, the agreement between theory and experiment is rather good. Actually a Γ increasing monotonically with energy would have considerably improved the fit. We can therefore conclude that a lifetime-broadened Franz-Keldysh effect can account for the major features of the optical field effects in rutile.

A few words should be said about the presence in the theory of an apparent second maximum at 3.60 eV. Although the experimental data do show a small inflection at this energy, we believe that the peak has been accidentally introduced by the large uncertainty in the values of ϵ_2 used in the calculation. At this very energy, ϵ_2 starts to deviate abruptly from zero.[15] We assume, therefore, that the inflection labeled E_2 and the small wiggles above it are associated with an independent critical point, most likely an M_0 parabolic threshold located at approximately 3.5 eV, as can be inferred by examination of the various curves of Fig. 10.

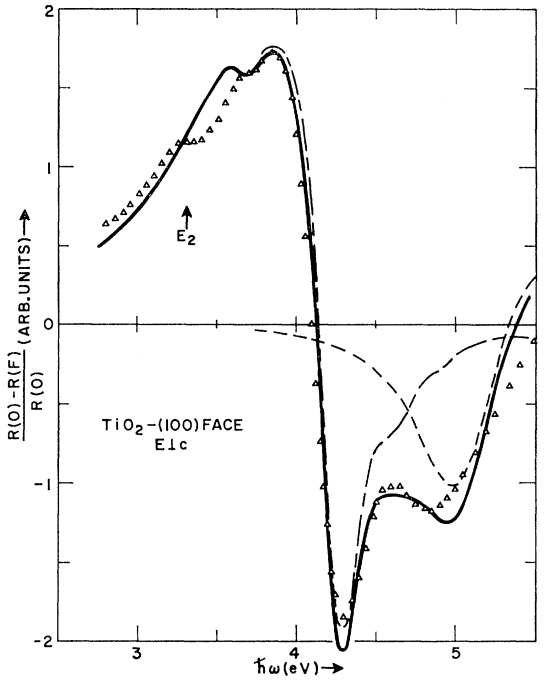

FIG. 11. Comparison between the experimental field-induced change in reflectance for a (100) face ($\mathbf{E}\perp c$) and the change calculated from the overlapping contributions of an M_1 transverse saddle-point located at 3.95 eV and an M_2 transverse located at 5.35 eV ($\hbar\Gamma_1=325$ meV, $\hbar\Gamma_2=570$ meV, $\hbar\Theta_1=190$ meV, $\hbar\Theta_2=270$ meV).

From the values of Γ used in the calculation, the relaxation time can be estimated to be at least 2×10^{-15} sec, which is rather close to the value predicted by transport experiments.[23] Γ appears to be the dominant parameter that determines the width of the ER spectra of rutile. In particular, since it is clear from Eq. (4) that the weight of Γ is larger for smaller Θ, structure due to critical points with large reduced mass might be almost completely washed out. In fact, it is surprising that the observed ER is so large despite the presence of strong lifetime-broadening effects. The possibility that exciton effects might greatly enhance the electromodulation of the optical constants should be considered.

Let us now turn to the case of a (100) face for $\mathbf{E}\|c$. A single critical point at A cannot account for the whole spectrum, as was implicitly assumed on the basis of absolute-reflectance results.[15] Although the major peak on the low-energy side of the spectrum can again be attributed primarily to an M_1 transverse saddle point located at ~4.0 eV, the high-energy side is apparently a mixture of at least two additional critical points. The contributions of the various edges are differently weighted for different orientation of the sample, as appears by comparison with Fig. 2 and Fig. 3. In

addition, all critical points undergo a small shift to lower energies in going from a (100) to a (110) surface. This occurs for both $\mathbf{E}\perp c$ and $\mathbf{E}\|c$. No attempt has been made to obtain a theoretical fit to the data of Fig. 4, taken on a face perpendicular to the c axis. Very qualitatively, it may be said that A_1 and A_2 are still the same types of critical points found in (100) and (110) spectra for $\mathbf{E}\perp c$. However, they appear to have moved much closer to each other. B_1 might be an M_3 or another M_1 transverse point at approximately 6.5 eV.

In conclusion, our results can provide detailed information on the band structure of rutile. Some theoretical knowledge would be highly desirable for the data to become completely meaningful. At this stage, we can only apply literally to rutile the band structure calculated by Kahn and Leyendecker for the perovskite-type titanates.[10] We propose that the direct band gap, occurring at Γ ($k=0$), is about 3.5 eV, while the optical gap at X is approximately 4 eV, with a possible splitting due to deviations from cubic symmetry.

VI. CONCLUSIONS

Critical points in the optical constants of TiO_2 have been determined by ER and EA measurements. Like the bands for the perovskite-type ferroelectrics, the ER bands in rutile have remarkably large magnitude and width, which suggests that this material should exhibit a strong electro-optic effect in the visible. Unlike the behavior of the tantalates, but consistent with that of $BaTiO_3$, only small shifts of the critical points have been observed in rutile when the dc field was varied, and the optical field effects could not be accounted for in terms of this mechanism alone. A good theoretical fit to the experimental data was obtained by assuming that the field-induced changes in the optical constants are due to a strongly lifetime-broadened Franz-Keldysh photon-assisted tunneling. Comparison of theory and experiment indicates that for electrons at energies higher than 1 eV above the bottom of the conduction band the relaxation time is at least 2×10^{-15} sec, a value which is close to that expected from the results of mobility measurements at room temperature.

ACKNOWLEDGMENTS

The authors are much indebted to D. Kahng for a number of profitable discussions, to J. R. Brews for a critical reading of the manuscript, and to E. O. Kane for valuable suggestions. Thanks are due to W. J. Sundburg and R. T. Hepplewhite for assistance in the preparation of the samples and to J. J. Rubin for providing the material used in this investigation. The authors are also grateful to M. Cardona for providing tables of the optical constants of rutile and to D. E. Aspnes and D. F. Blossey for allowing us the use of their computer subroutines for the generation of the Airy function and of its derivative.